Supporting Information

Hickman et al. 10.1073/pnas.0912279107

SI Materials and Methods

Experimental Design. Three sites were selected in Madison County, Georgia. Two sites were located on private property along Buford Carey Road (34.147, −83.326 and 34.145, −83.324) and one on private property along Stone Stewart Road (34.095, −83.309). Understanding the real-world ecosystem impacts of kudzu invasion requires field studies that are necessarily less controlled than manipulative experiments (1). Within each site, we established one plot within an area invaded by kudzu and a second in an adjacent area (within ≈20 m) that was not invaded. To minimize the chances that differences in land use history or other factors could confound the effects of kudzu invasion on soils, we located each pair of invaded and uninvaded plots within 30 m of one another and made sure that each plot pair shared similar land use histories, slopes, aspects, and soils.

The soils at all three sites were well-drained Madison sandy loam, with some variation in slope among sites. At the first Buford Carey site ("Carey blackberry"), the invaded and uninvaded plots were located on an east-facing 10–15% slope. Plots at the second Buford Carey site ("Carey Pasture") were located on a northeast-facing 6–10% slope, whereas plots at the Stone Stewart site ("Wilson Elder") were located on south-facing 6–10% slopes. Aerial photos from the Digital Library of Georgia, which collects aerial photography of Madison County produced by the Agricultural Stabilization and Conservation Service, were used to determine the land-use history of the sites (2). The first Buford Carey site is located in an area that appears shrubby at least as far back as 1951; no sign of agricultural activity is apparent at this site. The second Buford Carey site is located on land that was used as pasture starting as far back as the 1940s. After 1973, the land was no longer managed, although one area abutting the kudzu patch was mowed occasionally. The Stone Stewart site was farmed at least until 1951, but farming in the plots ceased before 1967.

Sample collection and preparation. Soil sampling was conducted from July 20 to 22 and September 15, 2007. At each sampling time, soil cores were taken from paired invaded and uninvaded plots on the same day. Four soil cores were taken from each plot, for a total of eight cores per site. The soil cores were taken at least 48 h after any rain event. Locations for soil cores were selected randomly in each plot. The top litter layer was removed, and a PVC pipe (5 cm internal diameter × 20 cm long) was driven 12 cm into the ground and removed with the core intact. The cores contained little or no organic layer, so they were not separated into different horizons before being placed in separate polyethylene bags. The cores were kept cool (packed on ice in coolers) until being transferred to a refrigerator in the laboratory. Most laboratory analyses were started within 3 days of soil collection, but the denitrification assays were usually conducted 4–6 days after sampling.

Soils were homogenized by hand in plastic bags, and major rocks, roots, and invertebrates were removed. Subsamples from each core were taken for laboratory analysis of moisture content, total C and N, initial nitrate and ammonium, microbial biomass, net mineralization and nitrification potential, and denitrification enzyme activity (details below). Soil moisture content (g H_2O g^{-1} dry soil) was determined by drying a subsample at 60 °C until soils were no longer decreasing in weight. Total carbon and nitrogen content of dried, ground samples was determined using a CE Flash EA 1112 Elemental Analyzer (CE Instruments).

Inorganic N pools. Inorganic N was extracted from soils by placing a 10-g subsample of soil from each core in a 120-mL polypropylene specimen cup with 50 mL 2 M KCl and shaking the cups for 60 min. The soils were allowed to settle for another 60 min after shaking. The KCl solution from each cup was filtered using Whatman #42 filter paper and stored below freezing in a 40-mL glass scintillation vial. Determinations of NO_3^-/NO_2^-–N and NH_4^+–N content were made using a Lachat autoanalyzer (Lachat Quickchem Systems). These measurements also represent the initial or "preincubation" inorganic N concentrations for the calculations of net N mineralization and net nitrification rates.

Net N mineralization and net nitrification. Concurrent with subsampling for the initial KCl extractions, a second 10-g subsample was taken from each homogenized core and placed in a 120-mL specimen cup, which in turn was placed in a mason jar and sealed with a gas-tight lid fitted with a rubber septum. The jars were incubated at 20–22 °C. After 10 days the specimen cups were removed, and inorganic N was extracted and analyzed as described above; these extractions represent the "postincubation" inorganic N content. Net mineralization was calculated as the difference in total inorganic N concentrations in the preincubation and postincubation extractions; net nitrification was calculated similarly, as the difference in NO_3^--N and NO_2^--N concentrations in pre- and postincubation soil extractions (4).

Soil microbial biomass. The determination of total microbial biomass was made using the chloroform fumigation incubation method (5, 6). A 10-g subsample of soil from each core was fumigated for 12–18 h. The 10-g samples of fumigated soils and a 0.1-g fresh soil inoculum from the same core were placed in a quart-sized mason jar and sealed with a gas-tight lid fitted with a rubber septum. A second 10.1-g fresh sample from the same core was sealed in a second mason jar. After incubating for 10 days at 20–22 °C, a 9-mL gas sample from the headspace of each mason jar was transferred to an evacuated glass vial. The vials were stored at room temperature until CO_2 concentrations were determined using a gas chromatograph fitted with a thermal conductivity detector. Headspace concentrations of CO_2-C were calculated. Microbial biomass-C was calculated as the CO_2-C per unit dry weight of soil in fumigated samples, divided by a constant (0.41) representing the fraction of biomass mineralized to CO_2.

Denitrification enzyme activity assays. We determined the denitrification potential of soils using the denitrification enzyme activity method (7). A slurry of soil and a medium containing a surfeit of nitrate and glucose was created, so that the denitrification process was limited only by the amount of denitrifying bacteria in the sample. Chloramphenicol, an inhibitor of microbial growth, was added to ensure the assay was measuring activity of the microbial community present in the soil at the time of sampling. A 5-g subsample was taken from each homogenized soil core and placed with 10 mL of medium into a 125-mL Erlenmeyer flask with a ground glass joint and sealed with a rubber stopper. The flasks were placed under negative pressure for 3 min, followed by a 1-min flush with N_2 gas. This process was repeated two more times to ensure that the soils were anaerobic. After the third flush with N_2, the flasks were vented, and 4 mL acetylene was added to each flask to inhibit the transformation of N_2O to N_2 by denitrifying bacteria. The flasks were placed on an orbital shaker, and 9-mL samples of the headspace of each flask were taken using a polypropylene syringe and transferred to evacuated gas vials after 1 and 3 h. The N_2O concentration of each vial was determined using a gas chromatograph fitted with an electron capture detector.

NO and N_2O emissions. Plots were sampled for NO and N_2O emissions from July 20 to 22, 2007. Air temperatures varied between 26 °C and 30 °C during sampling, and soil temperatures varied between 20 °C and 25°C; within each plot pair, soil temperatures

were higher on average in uninvaded plots than in invaded plots during sampling. Gas measurements for each set of paired uninvaded and invaded plots were conducted on the same day, and all sampling was conducted between 10:00 AM and 6:00 PM to limit any variation in temperature between plots. In each plot, four beveled, Teflon-coated PVC rings (25.5 cm diameter) were randomly inserted several centimeters into the soil, for eight chambers total per site. At least 30 min after inserting the ring, a Teflon-coated, molded PVC chamber top fitted with a gas-sampling port was inserted over the ring and made gas-tight. Emissions of NO were measured in situ using a portable chemiluminescent detector equipped with a CrO_3 filter that converts all NO to NO_2 (Unisearch Associates, Concord, ON, Canada) (8). Standard curves were conducted in the field before and after measurements were made from the four chambers in each plot using a standard gas with a known NO_2 concentration (0.0992 ppm; Scott-Marrin). Ambient NO_2 concentrations were low but detectable, so NO_2 concentrations within the chamber were measured immediately before and after NO measurements to measure the consumption of ambient NO_2 by soils, which was assumed to be linear. NO emissions were measured as the linear increase in NO concentrations in the chamber over 4 min and were corrected for the consumption of ambient NO_2 during that 4-min period (9).

To measure N_2O emissions, a Teflon-coated, molded PVC chamber top fitted with a septum was placed over each ring and made gas-tight. Using polypropylene syringes, 9-mL gas samples were taken from the chamber at 0, 10, 20, and 30 min and transferred to evacuated glass vials. The vials were stored at room temperature until analysis for N_2O using a gas chromatograph fitted with an electron capture detector. The N_2O flux was calculated using the linear increase in N_2O concentration, the chamber volume, and the soil surface area.

Statistical Analysis. Analyses of the NO and N_2O fluxes were conducted using split-plot ANOVA, including site and kudzu invasion as whole and within-plot factors, respectively. For the soil N and microbial variables, which were taken both in July and September, we conducted separate split-plot ANOVAs at each time point to avoid nonindependence of samples within any single analysis. A repeated-measures approach was not strictly possible because soil sampling was randomized separately at each sampling time. As with the trace gas analysis, site was included as a whole-plot factor and kudzu invasion as a within-plot factor. In all analyses, data were transformed as necessary to meet the assumptions of ANOVA. We used one-tailed tests for analyses of NO fluxes, N_2O fluxes, and measurements of N cycling and pools.

Ozone Sensitivity Analysis. To investigate the potential effects of a kudzu invasion on regional ozone levels, we used the global chemical transport model GEOS-Chem, focusing on the summer season (June–August) when ozone levels are highest. The GEOS-Chem model has been extensively used in past studies on tropospheric ozone and its precursors, both globally (10–13) and for the United States (14–19). We used GEOS-Chem version 8.01.01 (http://www.as.harvard.edu/chemistry/trop/geos/) with the meteorological input from the National Aeronautics and Space Administration/Goddard Institute for Space Studies general circulation model. A more detailed model description is available from Wu et al. (13, 19).

The soil NO_x inventory in the standard version of GEOS-Chem follows the review/synthesis of Yienger and Levy (20). For this study, we scaled the calculated soil NO_x emission in the southeastern United States according to Davidson et al.'s estimated NO fluxes in this region (21). We followed the Intergovernmental Panel on Climate Change A1B scenario for 2050 in which the United States NO_x emissions from fossil fuel are projected to decrease by 40% owing to technological improvements. The meteorology was simulated for 2050, which enhances the soil NO_x emissions by 8% compared with 2000 owing to higher temperatures (19). NO flux from nonagriculture soils accounts for approximately one third of the total soil NO emissions over the Southeast (21). In our sensitivity test, we assumed full kudzu coverage over the nonagriculture land area over the southeastern United States. Assuming that the increases in NO fluxes observed at our Georgia sites are representative of the impacts of kudzu across the southeastern United States, this full kudzu coverage increases total soil NO_x emission by 28%. We set 70 ppb as the threshold for signifying an ozone episode; previous research has shown that use of a 70 ppb threshold in a similar coarse-grid chemistry model provided good statistics for the occurrence of ozone episodes when compared with observations (15).

1. Ashton IW, Hyatt LA, Howe KM, Gurevitch J, Lerdau MT (2005) Invasive species accelerate decomposition and litter nitrogen loss in a mixed deciduous forest. *Ecol Appl* 15:1263–1272.
2. US Department of Agriculture (1944–1980) *Georgia Aerial Photographs* (Digital Library of Georgia, Athens, GA).
3. Paul EA, Clark FE (1996) *Soil Microbiology and Biochemistry* (Academic Press, San Diego).
4. Matson PA, Vitousek PM, Ewel JJ, Mazzarino MJ, Robertson GP (1987) Nitrogen transformations following tropical forest felling and burning on a volcanic soil. *Ecology* 68:491–502.
5. Jenkinson DS, Powlson DS (1976) Effects of biocidal treatments on metabolism in soil 1. Fumigation with chloroform. *Soil Biol Biochem* 8:167–177.
6. Voroney RP, Paul EA (1984) Determination of Kc And Kn in situ for calibration of the chloroform fumigation incubation method. *Soil Biol Biochem* 16:9–14.
7. Smith MS, Firestone MK, Tiedje JM (1978) Acetylene inhibition method for short-term measurement of soil denitrification and its evaluation using N-13. *Soil Sci Soc Am J* 42: 611–615.
8. Matson PA, Billow C, Hall S, Zachariassen J (1996) Fertilization practices and soil variations control nitrogen oxide emissions from tropical sugar cane. *J Geophys Res* 101:18533–18545.
9. Hall SJ, Matson PA (2003) Nutrient status of tropical rain forests influences soil N dynamics after N additions. *Ecol Monogr* 73:107–129.
10. Bey I, et al. (2001) Global modeling of tropospheric chemistry with assimilated meteorology: Model description and evaluation. *J Geophys Res* 106:23073–23095.
11. Martin RV, et al. (2002) Interpretation of TOMS observations of tropical tropospheric ozone with a global model and in situ observations. *J Geophys Res,* 107:4351.
12. Sauvage B, et al. (2007) Remote sensed and in situ constraints on processes affecting tropical tropospheric ozone. *Atmos Chem Phys* 7:815–838.
13. Wu SL, et al. (2007) Why are there large differences between models in global budgets of tropospheric ozone? *J Geophys Res,* 112:D05302.
14. Fiore A, et al. (2003) Variability in surface ozone background over the United States: Implications for air quality policy. *J Geophys Res,* 108:4787.
15. Fiore AM, et al. (2002) Background ozone over the United States in summer: Origin, trend, and contribution to pollution episodes. *J Geophys Res,* 107:4275.
16. Fiore AM, Jacob DJ, Mathur R, Martin RV (2003) Application of empirical orthogonal functions to evaluate ozone simulations with regional and global models. *J Geophys Res* 108:4431.
17. Hudman RC, et al. (2004) Ozone production in transpacific Asian pollution plumes and implications for ozone air quality in California. *J Geophys Res* 109:D23S10.
18. Hudman RC, et al. (2007) Surface and lightning sources of nitrogen oxides over the United States: Magnitudes, chemical evolution, and outflow. *J Geophys Res,* 112:D12S05.
19. Wu SL, et al. (2008) Effects of 2000-2050 global change on ozone air quality in the United States. *J Geophys Res,* 113:D06302.
20. Yienger JJ, Levy H (1995) Empirical model of global soil biogenic NOx emissions. *J Geophys Res* 100:11447–11464.
21. Davidson EA, Potter CS, Schlesinger P, Klooster SA (1998) Model estimates of regional nitric oxide emissions from soils of the southeastern United States. *Ecol Appl* 8: 748–759.

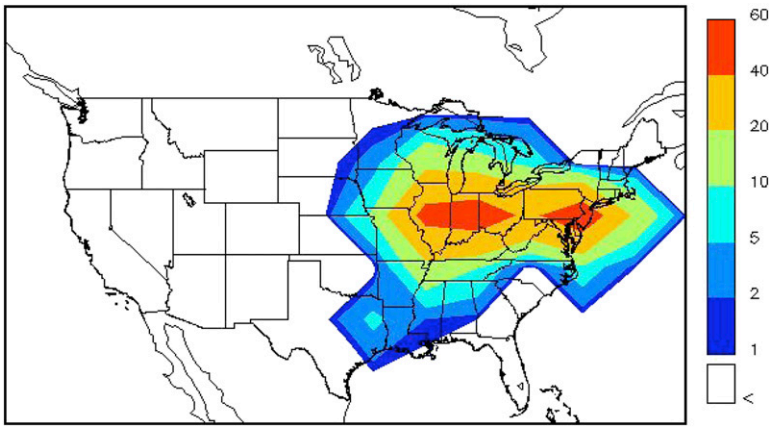

Fig. S1. Number of days with daily maxima 8-h ozone exceeding 70 ppb during summer (June–August) in the absence of NO_x emissions from kudzu for a nine-state region in the southeastern United States. Results are from the GEOS-Chem model for 2050's climate conditions under the A1B scenario.

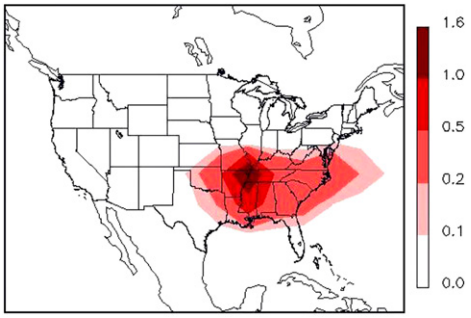

Fig. S2. Calculated change in summer (June–August) average surface ozone (in ppb) due to the 28% increase in soil NO_x emissions accompanying kudzu invasion of all nonagricultural, nonurban soils in a nine-state region. Results are from the GEOS-Chem model for 2050's climate conditions.